Higgs boson production in the $U(1)_{B-L}$ model at the ILC

Jinzhong Han[1],* Bingfang Yang[2],† Ning Liu[2],‡ and Jitao Li[1]

[1] *School of Physics and Telecommunications Engineering, Zhoukou Normal University, Henan, 466001, China*

[2] *College of Physics and Electronic Engineering, Henan Normal University, Xinxiang 453007, China*

Abstract

In the framework of the minimal $U(1)_{B-L}$ extension of the Standard Model, we investigate the Higgs boson production processes $e^+e^- \to ZH$, $e^+e^- \to \nu_e\bar{\nu}_e H$, $e^+e^- \to t\bar{t}H$, $e^+e^- \to ZHH$ and $e^+e^- \to \nu_e\bar{\nu}_e HH$ at the International Linear Collider (ILC). We present the production cross sections, the relative corrections and compare our results with the expected experimental accuracies for Higgs decay channel $H \to b\bar{b}$. In the allowed parameter space, we find that the effects of the three single Higgs boson production processes might approach the observable threshold of the ILC, and that the Higgs signal strengths $\mu_{b\bar{b}}$ of the two double Higgs boson production processes are all out of the observable threshold of the ILC so that the effects will be difficult to be observed at the ILC.

PACS numbers: 14.80.Ec,12.15.Lk,12.60.-i

*Electronic address: hanjinzhong@zknu.edu.cn

†Electronic address: yangbingfang@htu.edu.cn

‡Electronic address: wlln@mail.ustc.edu.cn

I. INTRODUCTION

In the summer of 2012, a bosonic resonance with a mass around 125 GeV was found at the Large Hadron Collider (LHC) by the ATLAS and CMS Collaborations [1, 2]. So far, its properties are compatible with the predictions of the Standard Model (SM) Higgs boson. While we know that the precision measurements of the properties of the Higgs boson at the LHC are severely challenged due to the complicated background. In addition, the current LHC data is limited, there are still large uncertainties about the couplings between the Higgs boson and the other SM particles [3] . However, another Higgs factory beside the LHC, such as the International Linear Collider (ILC) [4, 5], can measure the properties of the Higgs boson with high accuracy due to its clean environment. In many cases, the ILC can significantly improve the LHC measurements.

The ILC technical design report has pointed that it is planed to measure Higgs boson at three center-of-mass (c.m.) energy: 250 GeV, 500 GeV and 1000 GeV. In the first stage for $\sqrt{s} = 250$ GeV, the precision Higgs program will start at the Higgs-strahlung process $e^+e^- \to ZH$, the cross section for this process is dominant at the low energy and has the maximum cross section at around $\sqrt{s} = 250$ GeV. In the second stage for $\sqrt{s} = 500$ GeV, the two very important processes $e^+e^- \to t\bar{t}H$ and $e^+e^- \to ZHH$ are become accessible. For the process $e^+e^- \to t\bar{t}H$, in which the top Yukawa coupling appears in the tree level for the first time at the ILC, it will play an important role for the precision measurements of the top quark Yukawa coupling. For the process $e^+e^- \to ZHH$, to which the triple Higgs boson coupling contributes in the tree level. This process will be crucial to understand the Higgs self-coupling and the electroweak symmetry breaking. In the third stage for $\sqrt{s} = 1000$ GeV, the processes $e^+e^- \to t\bar{t}H$, $e^+e^- \to \nu_e\bar{\nu}_eH$ and $e^+e^- \to \nu_e\bar{\nu}_eHH$ are involved. The channels $t\bar{t}H$ and $\nu_e\bar{\nu}_eH$ have large cross section in such energy stages. The channel $\nu_e\bar{\nu}_eHH$ can be used together with the ZHH process to improve the measurement of the Higgs self-coupling. So far, many relevant works mentioned above have been extensively studied in the context of the SM [6] and some new physics models [7–9].

The minimal $B-L$ extension of the SM is based on the structure $SU(3)_C \times SU(2)_L \times U(1)_Y \times U(1)_{B-L}$ gauge symmetry, in which the SM gauge has a further $U(1)_{B-L}$ group related to the Baryon minus Lepton $(B-L)$ gauged number [10]. It was known that this

model is in agreement with the current experimental results of the light neutrino masses and their large mixing. The $B-L$ model predicted some new particles beyond the SM, such as the new heavy gauge bosons, the heavy neutrino and the heavy neutral Higgs boson. In addition, some couplings of the Higgs boson in the $B-L$ model are modified with respect to the SM. These new effects will alter the property of the SM Higgs boson and influence various SM Higgs boson processes, making the model phenomenologically rich and testable at the LHC and the ILC [11–21]. In this paper, we mainly study the Higgs boson production processes $e^+e^- \to ZH$, $e^+e^- \to \nu_e\bar{\nu_e}H$, $e^+e^- \to e^+e^-H$, $e^+e^- \to t\bar{t}H$, $e^+e^- \to ZHH$ and $e^+e^- \to \nu_e\bar{\nu_e}HH$ in the $B-L$ model at the ILC.

The paper is organized as follows. In Sec.II we briefly review the basic content of the $B-L$ model related to our work. In Sec.III and Sec.IV we respectively investigate the Higgs boson production processes and the Higgs signal strengths in the $B-L$ model at the ILC. Finally, we give a summary in Sec.V.

II. A BRIEF REVIEW OF THE B-L MODEL

Here we will briefly review the ingredients relevant to our calculations, the detailed description of the $B-L$ model can be found in Refs. [11, 14]. For the $B-L$ model, it is one of the minimal extensions of the SM [22–26]. The Lagrangian for the fermionic and kinetic sectors are given by

$$\begin{aligned}\mathcal{L}_{B-L} &= i\,\bar{l}D_\mu\gamma^\mu l + i\,\bar{e}_R D_\mu\gamma^\mu e_R + i\,\bar{\nu}_R D_\mu\gamma^\mu\nu_R \\ &\quad -\frac{1}{4}W_{\mu\nu}W^{\mu\nu} - \frac{1}{4}B_{\mu\nu}B^{\mu\nu} - \frac{1}{4}C_{\mu\nu}C^{\mu\nu}. \end{aligned} \tag{1}$$

The covariant derivative D_μ is different from the SM one by the term $ig'Y_{B-L}C_\mu$, where g' is the $U(1)_{B-L}$ gauge coupling constant, Y_{B-L} is the $B-L$ charge, and $C_{\mu\nu} = \partial_\mu C_\nu - \partial_\nu C_\mu$ is the field strength of the $U(1)_{B-L}$.

The Lagrangian for the Higgs and Yukawa sectors are given by

$$\begin{aligned}\mathcal{L}_{B-L} &= (D^\mu\phi)(D_\mu\phi) + (D^\mu\chi)(D_\mu\chi) - V(\phi,\chi) \\ &\quad -\Big(\lambda_e\bar{l}\phi e_R + \lambda_\nu\bar{l}\tilde{\phi}\nu_R + \frac{1}{2}\lambda_{\nu_R}\bar{\nu^c}_R\chi\nu_R + h.c.\Big). \end{aligned} \tag{2}$$

The $U(1)_{B-L}$ and $SU(2)_L\times U(1)_Y$ gauge symmetries can be spontaneously broken by a SM singlet complex scalar field χ and a complex $SU(2)$ doublet of scalar fields ϕ, respectively.

The scalar potential $V(\phi,\chi)$ is given by

$$\begin{aligned} V(\phi,\chi) \;=\; & m_1^2\phi^\dagger\phi + m_2^2\chi^\dagger\chi + \lambda_1(\phi^\dagger\phi)^2 + \lambda_2(\chi^\dagger\chi)^2 \\ & +\lambda_3(\chi^\dagger\chi)(\phi^\dagger\phi). \end{aligned} \tag{3}$$

For the potential to be bounded from below, the couplings λ_1, λ_2 and λ_3 should be related with $4\lambda_1\lambda_2 - \lambda_3 > 0, \lambda_1 \geq 0, \lambda_2 \geq 0$. The vev's, $|\langle\phi\rangle| = v/\sqrt{2}$ and $|\langle\chi\rangle| = v'/\sqrt{2}$, are then given by

$$v^2 = \frac{4\lambda_2 m_1^2 - 2\lambda_3 m_2^2}{\lambda_3^2 - 4\lambda_1\lambda_2}, \qquad v'^2 = \frac{-2(m_1^2 + \lambda_1 v^2)}{\lambda_3}. \tag{4}$$

v and v' are the electroweak symmetry breaking scale and the $B-L$ symmetry breaking scale.

In addition, after the electroweak symmetry breaking, one obtains the mass of the gauge bosons

$$\begin{aligned} m_\gamma &= 0, \\ m_{W^\pm} &= \frac{1}{2}vg, \\ m_Z &= \frac{v}{2}\sqrt{g^2 + g_1^2}, \\ m_{Z'} &= 2v'g'. \end{aligned} \tag{5}$$

where g and g_1 are the $SU(2)_L$ and $U(1)_Y$ gauge coupling constant. However, the ratio of Z' mass to that of its couplings is constrained from the most recent limit at LEP [27]

$$m_{Z'}/g' > 7 \text{ TeV}. \tag{6}$$

The mixing between the SM complex $SU(2)_L$ doublet and complex scalar singlet is controlled by the coupling λ_3 as shown in Eq. 3. This mixing can be expressed by the mass matrix ϕ and χ

$$\frac{1}{2}m^2(\phi,\chi) = \begin{pmatrix} \lambda_1 v^2 & \frac{\lambda_3}{2}vv' \\ \frac{\lambda_3}{2}vv' & \lambda_2 v'^2 \end{pmatrix}. \tag{7}$$

Therefore, the mass eigenstates fields H and H' are given by

$$\begin{pmatrix} H \\ H' \end{pmatrix} = \begin{pmatrix} \cos\alpha & -\sin\alpha \\ \sin\alpha & \cos\alpha \end{pmatrix} \begin{pmatrix} \phi \\ \chi \end{pmatrix}, \tag{8}$$

where the mixing angle α is defined by

$$\tan 2\alpha = \frac{|\lambda_3| v v'}{\lambda_1 v^2 - \lambda_2 v'^2}. \tag{9}$$

The masses of H and H' are given by

$$m^2_{H,H'} = \lambda_1 v^2 + \lambda_2 v'^2 \mp \sqrt{(\lambda_1 v^2 - \lambda_2 v'^2)^2 + \lambda_3^2 v^2 v'^2}. \tag{10}$$

Here, H and H' are light and heavy Higgs bosons, respectively.

Because of the mixing between the two Higgs bosons H and H', the usual couplings among the SM-like Higgs H boson and the SM fermions and gauge bosons are modified. Additionally, there are new couplings among the extra Higgs H' and the SM particles, which will lead to a different Higgs phenomenology from the SM. The relevant Feynman rules involved in our calculations are given in [15, 18].

III. HIGGS PRODUCTIONS IN THE B-L MODEL AT ILC

In our numerical calculations, we take the SM parameters as: m_t =172.4 GeV, $\sin^2\theta_W$ =0.23126, m_Z =91.187 GeV, m_W =80.389 GeV, m_H =125.9 GeV, $\alpha(m_Z)$=1/128 [28]. For the parameters in the $B-L$ model, the mixing angle α, the masses $m_{Z'}$, $m_{H'}$ and m_{ν_H} are involved. The Ref. [29] has discussed the constraints on these parameters from two respects of experiment and theory, and points out that $\sin\alpha \leq 0.36$, $m_{Z'} \geq 1830$ GeV, $m_{\nu_H} \sim 500$ GeV, $m_{H'} \geq 125$ GeV. In the following calculation, we vary $\sin\alpha$ and $m_{Z'}$ in the range of $0.1 \leq \sin\alpha \leq 0.4$, 1000 GeV $\leq m_{Z'} \leq$ 3000 GeV, and we pick two typical values of $m_{\nu_H} = 500$ GeV, $m_{H'} = 500$ GeV. All the numerical results are done by using CalcHEP package [30].

A. Single Higgs boson productions

In the $B-L$ model, the lowest-order Feynman diagrams of the single Higgs boson production processes $e^+e^- \to ZH$, $e^+e^- \to \nu_e\bar{\nu}_e H$ and $e^+e^- \to t\bar{t}H$ are shown in Fig.1 and Fig.2. In comparison with the SM, we can see that these three processes receive the additional contributions arising from the heavy gauge boson Z' and the modified couplings of HXX at the tree-level in the $B-L$ model.

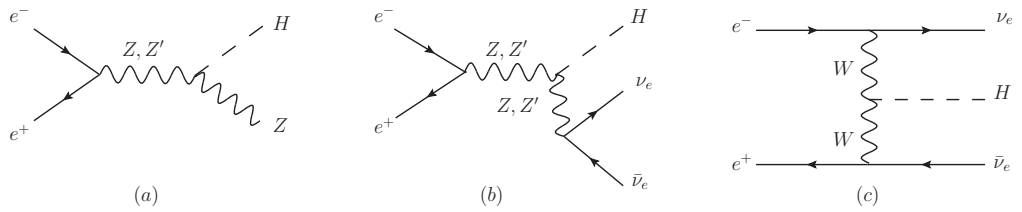

FIG. 1: Lowest-order Feynman diagrams for $e^+e^- \to ZH$(a) and $e^+e^- \to \nu_e\bar{\nu}_e H$(b,c) in the $B-L$ model.

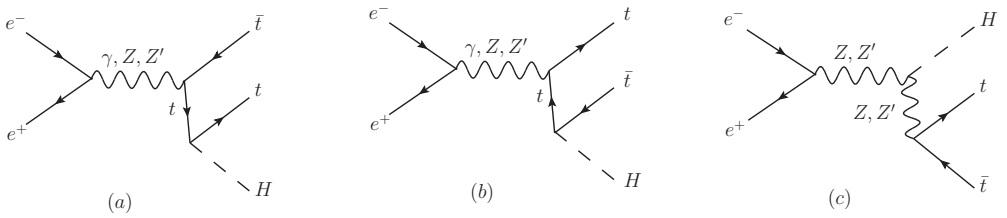

FIG. 2: Lowest-order Feynman diagrams for $e^+e^- \to t\bar{t}H$ in the $B-L$ model.

In Fig.3, we show the production cross section σ of these three processes as functions of the c.m. energy $\sqrt{s}$ in the SM and $B-L$ model. We can see that the process $e^+e^- \to ZH$ reaches its maximum at about 250 GeV. The $\nu_e\bar{\nu}_e H$ production cross sections increase with the c.m. energy and can take over that of the ZH process at $\sqrt{s} \geq 500$ GeV. Similar to that of the $e^+e^- \to ZH$, the $t\bar{t}H$ production cross sections increase firstly and then decrease and reaches its maximum at about 800 GeV. The cross sections of these three

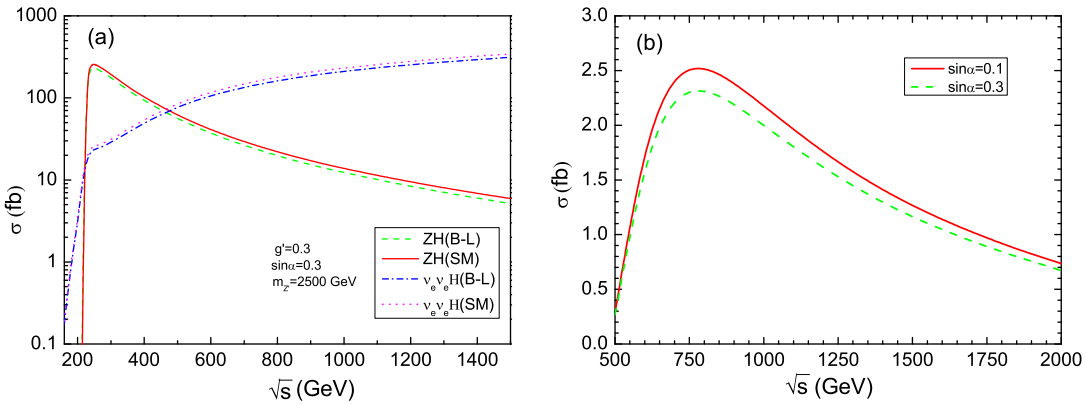

FIG. 3: The production cross section σ for the process $e^+e^- \to ZH$, $e^+e^- \to \nu_e\bar{\nu}_e H$ (a) and $e^+e^- \to t\bar{t}H$ (b) versus the c.m. energy $\sqrt{s}$ in the SM and $B-L$ model.

production processes in the $B-L$ model are all lower than the cross sections in the SM.

Considering the polarization of the initial electron and positron beams, the cross section of a process can be expressed as [31]

$$\begin{aligned}\sigma(P_{e^-},P_{e^+}) &= \frac{1}{4}[(1+P_{e^-})(1+P_{e^+})\sigma_{RR}+(1-P_{e^-})(1-P_{e^+})\sigma_{LL} \\ &+(1+P_{e^-})(1-P_{e^+})\sigma_{RL}+(1-P_{e^-})(1+P_{e^+})\sigma_{LR}],\end{aligned} \tag{11}$$

where P_{e^-} and P_{e^+} are the polarization degree of the electron and positron beam, respectively. As in Ref. [5], we assume $P(e^-,e^+)=(-0.8,0.3)$ at $\sqrt{s}$=250, 500 GeV and $P(e^-,e^+)=(-0.8,0.2)$ at $\sqrt{s}$=1000 GeV in our calculations.

In Fig. 4 and Fig. 5 we show the relative correction $\Delta\sigma/\sigma=(\sigma_{B-L}-\sigma_{SM})/\sigma_{SM}$ for the three production channels as a function of $m_{Z'}$ for $\sqrt{s}=250,500,1000$ GeV at the ILC with polarized beams. For these three processes, we can see that the values of the relative corrections decrease with the $m_{Z'}$ increasing, the relative corrections are all negative and the magnitude of deviation is insensitive to the $m_{Z'}$. On the contrary, the relative corrections are sensitive to the sinα and become larger in size for larger sinα.

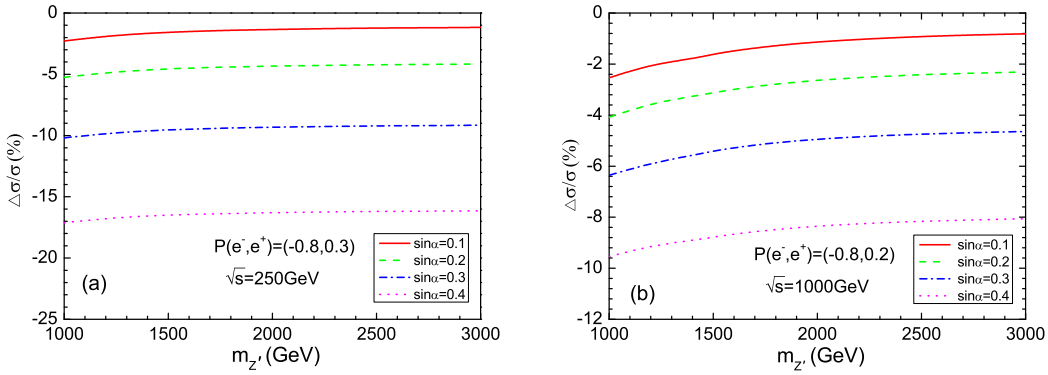

FIG. 4: The relative correction $\Delta\sigma/\sigma$ for the process $e^+e^-\to ZH$ at $\sqrt{s}=250$ GeV (a) and $e^+e^-\to\nu_e\bar{\nu}_eH$ at $\sqrt{s}=1000$ GeV (b) versus the mass $m_{Z'}$ in the $B-L$ model.

At the ILC with $\sqrt{s}=250$ GeV , the total SM electroweak correction for the ZH production process is about 5% [32]. The expected accuracies for ZH and $\nu_e\bar{\nu}_eH$ cross section are about $2.0-2.6\%$ and $2.2-11\%$ for $m_H=125$ GeV [5]. In addition, the expected accuracies for $t\bar{t}H$ process, an even more remarkable precision of 6.3% may be achieved at the ILC for $\sqrt{s}=1000$ GeV [5]. Thus, for the larger sinα, the $B-L$

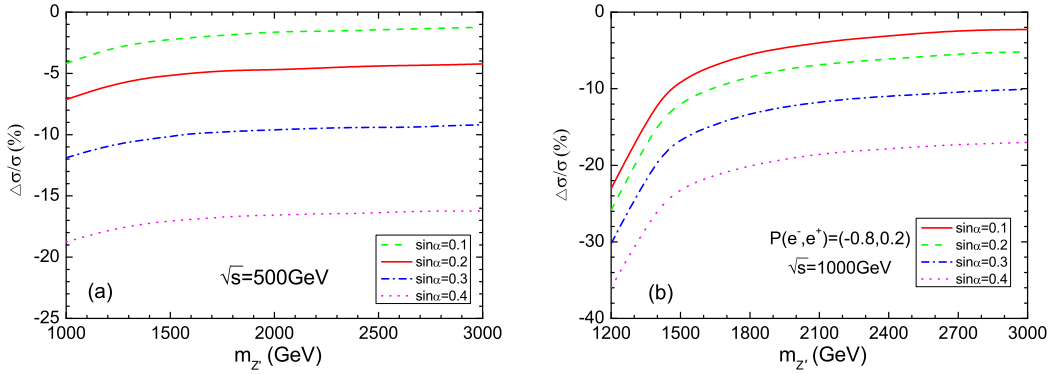

FIG. 5: The relative correction $\Delta\sigma/\sigma$ for the process $e^+e^- \to t\bar{t}H$ versus the mass $m_{Z'}$ for $\sqrt{s} = 500$ GeV (a) and $\sqrt{s} = 1000$ GeV (b) in the $B - L$ model.

model effects on these three processes might be observed in the future high precision ILC experiments.

B. Double Higgs boson productions

At the ILC, the main triple Higgs boson coupling can be studied through the double Higgs-strahlung off Z bosons process $e^+e^- \to ZHH$ and double Higgs fusions process $e^+e^- \to \nu_e\bar{\nu}_e HH$. The relevant Feynman diagrams are shown in Fig. 6 and Fig. 7. The cross sections for the two processes in the SM and the $B - L$ model are plotted as a function of c.m. energy $\sqrt{s}$ for $g' = 0.3$, $\sin\alpha = 0.3$, $m_{Z'} = 2500$ GeV in Fig. 8. The cross section for the process $e^+e^- \to ZHH$ reaches its maximum at around 500 GeV. It is noteworthy that the process $e^+e^- \to \nu_e\bar{\nu}_e HH$ will become sizable at $\sqrt{s} = 1000$ GeV. This reaction can be used together with the $e^+e^- \to ZHH$ process to improve the measurement of the Higgs self-coupling. We can also find that they have a similar trend in the SM and the $B - L$ model.

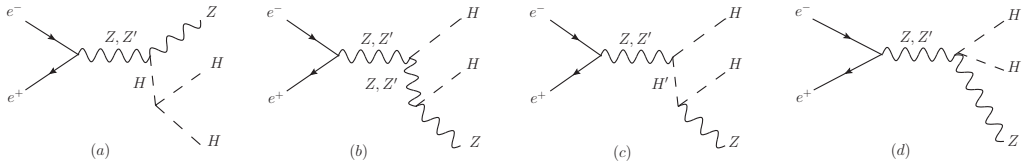

FIG. 6: Lowest-order Feynman diagrams for $e^+e^- \to ZHH$ in the $B - L$ model.

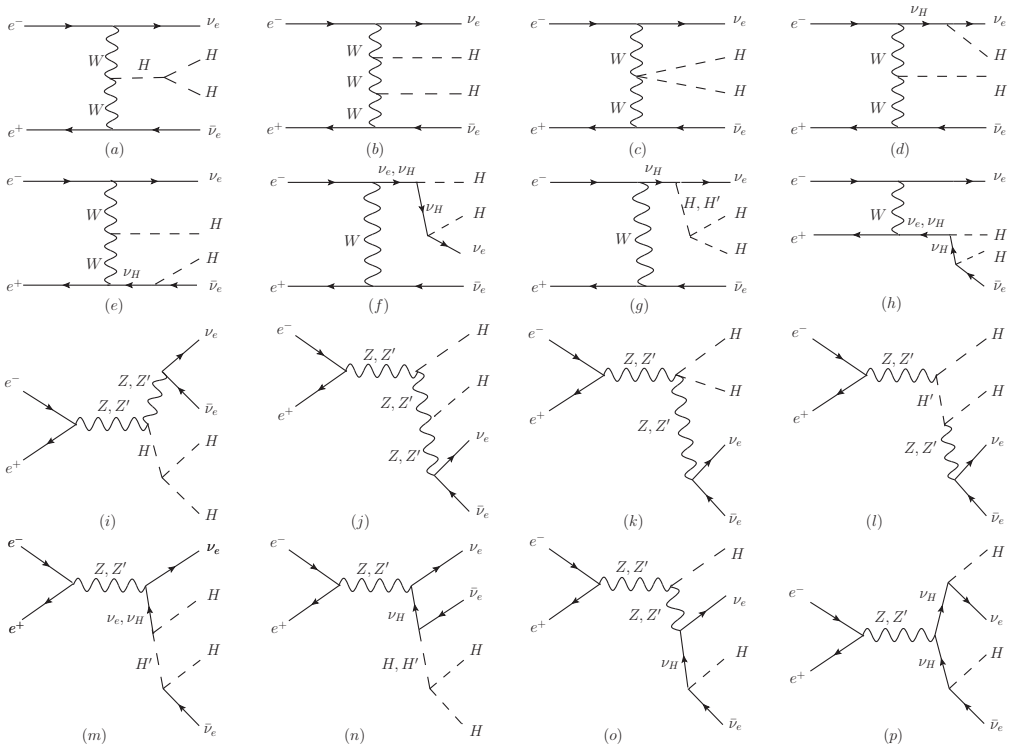

FIG. 7: Lowest-order Feynman diagrams for $e^+e^- \to \nu_e\bar{\nu}_e HH$ in the $B-L$ model.

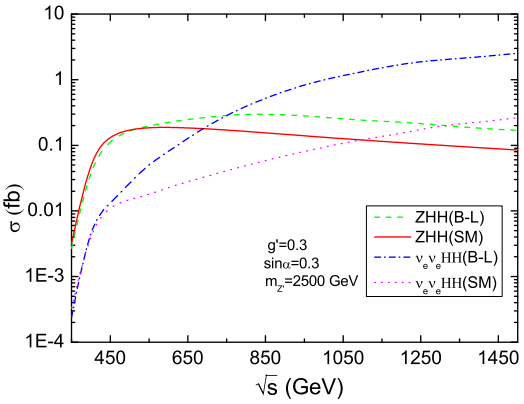

FIG. 8: The production cross section σ for the processes $e^+e^- \to ZHH$ and $e^+e^- \to \nu_e\bar{\nu}_e HH$ versus the c.m. energy $\sqrt{s}$ in the $B-L$ model.

In Fig. 9, we show the relative corrections of these two double Higgs production processes as a function of $m_{Z'}$ for $\sqrt{s} = 500, 1000$ GeV with polarized beams at the ILC. One can see that with the increasing of the mass parameter $m_{Z'}$, the values of the relative corrections are all negative and become smaller, the behavior is similar to that of the single Higgs produce processes mentioned above. The Refs [33, 34] suggest that the expected

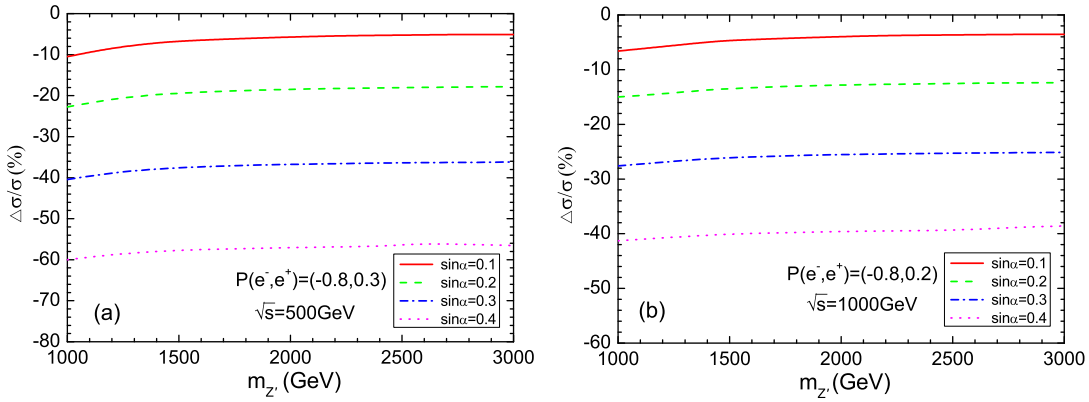

FIG. 9: The relative correction $\Delta\sigma/\sigma$ for the processes $e^+e^- \to ZHH$ at $\sqrt{s} = 500$ GeV (a) and $e^+e^- \to \nu_e\bar{\nu}_e HH$ at $\sqrt{s} = 1000$ GeV (b) versus the mass $m_{Z'}$ in the $B-L$ model.

accuracy for the HHH coupling could be reached to 50% through $pp \to HH \to bb\gamma\gamma$ at the HL-LHC with $\mathcal{L}$=3000 fb^{-1}, and this accuracy may be further improved to be around 13% at the ILC with $\sqrt{s}$=1000 GeV [33]. So, the effects of the $B-L$ model on these two processes might be observed at the ILC.

IV. THE HIGGS SIGNAL STRENGTHS IN THE B-L MODEL

In order to provide more information for probing the $B-L$ model, we also give the Higgs signal strengths in the $B-L$ model. Considering the Higgs boson decay mode, the Higgs signal strengths can be defined as

$$\mu_i = \frac{\sigma_{B-L} \times BR(H \to i)_{B-L}}{\sigma_{SM} \times BR(H \to i)_{SM}}, \tag{12}$$

where i denotes a possible final state of the SM fermion and boson pairs. The expected accuracies for cross section times branching ratio measurements for the 125 GeV Higgs boson at the ILC are shown in Table I. It is easy to see that the $b\bar{b}$ channel is more easily accessible than other channels. So, we only consider the decay mode $H \to b\bar{b}$ in the following section.

In Fig. 10, we show the dependence of the Higgs signal strengths $\mu_{b\bar{b}}$ on the parameters $m_{Z'}$ and sinα for the process $e^+e^- \to ZH$ with polarized beams. From Table I we can see that the 1.1(1.8)% accuracy for this mode are expected at $\sqrt{s} = 250(500)$ GeV. When

TABLE I: Expected accuracies for cross section times branching ratio measurements for the 125 GeV Higgs boson [5].

	$\Delta(\sigma \cdot BR)/(\sigma \cdot BR)$								
$\mathcal{L}$ and $\sqrt{s}$ (P_{e^-}, P_{e^+})	250 fb^{-1} at 250 GeV (-0.8, +0.3)		500 fb^{-1} at 500 GeV (-0.8, +0.3)				1000 fb^{-1} at 1000 GeV (-0.8, +0.2)		
mode	ZH	$\nu_e\bar{\nu}_e H$	ZH	$\nu_e\bar{\nu}_e H$	$t\bar{t}H$	ZHH	$\nu_e\bar{\nu}_e H$	$t\bar{t}H$	$\nu_e\bar{\nu}_e HH$
$h \to b\bar{b}$	1.1%	10.5%	1.8%	0.66%	35%	64%	0.47%	8.7%	38%
$h \to c\bar{c}$	7.4%	-	12%	6.2%	-	-	7.6%	-	-
$h \to gg$	9.1%	-	14%	4.1%	-	-	3.1%	-	-
$h \to WW^*$	9.1%	-	9.2%	2.6%	-	-	3.3%	-	-
$h \to \tau^+\tau^-$	4.2%	-	5.4%	14%	-	-	3.5%	-	-
$h \to ZZ^*$	19%	-	25%	8.2%	-	-	4.4%	-	-
$h \to \gamma\gamma$	29-38%	-	29-38%	20-26%	-	-	7-10%	-	-

$\sin\alpha > 0.1$, $m_{Z'} \geq 2000$ GeV, the contributions of the $B-L$ model might be detected by the measurement of the $b\bar{b}$ signal rate in the future ILC experiments.

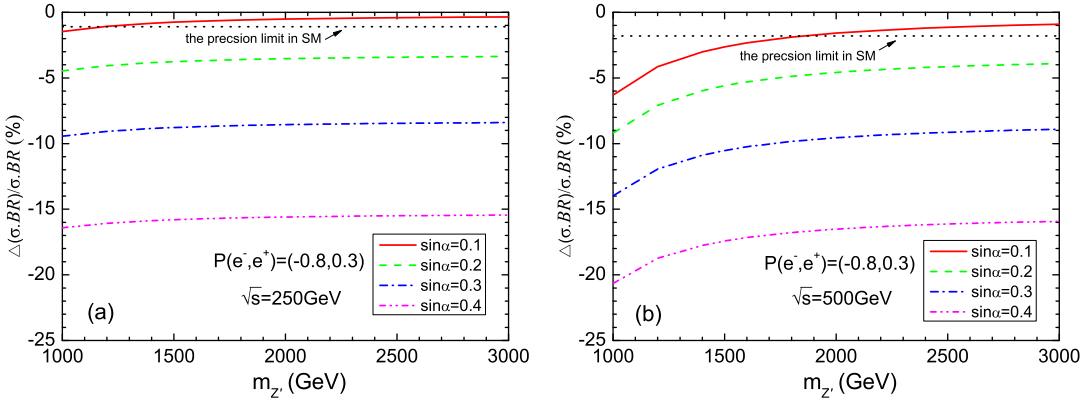

FIG. 10: Higgs signal strengths $\mu_{b\bar{b}}$ for the process $e^+e^- \to ZH$ versus the mass $m_{Z'}$ for $\sqrt{s} = 250$ GeV (a) and $\sqrt{s} = 500$ GeV (b) in the $B-L$ model.

In Fig. 11 and Fig. 12, we show the dependence of the Higgs signal strengths $\mu_{b\bar{b}}$ on the parameter $m_{Z'}$ and $\sin\alpha$ for the processes $e^+e^- \to \nu_e\bar{\nu}_e H$ and $e^+e^- \to t\bar{t}H$ with polarized beams, respectively. From Table I we know that the 0.66(0.47)% accuracy is

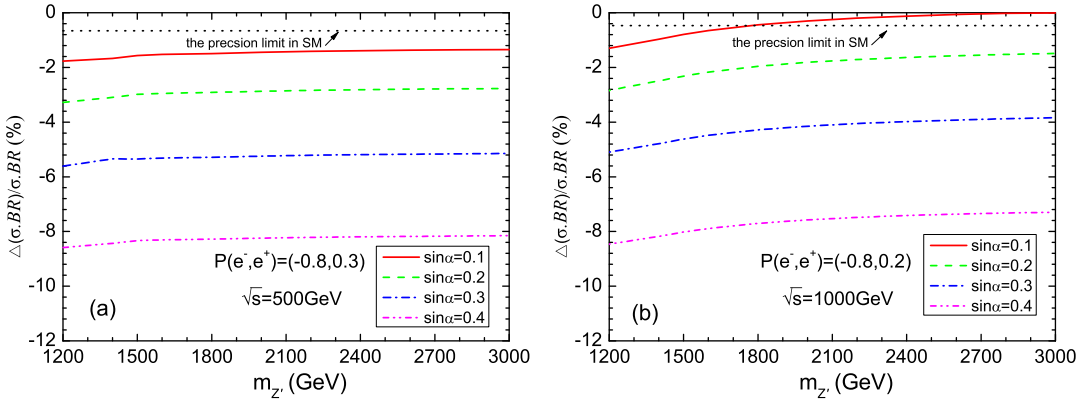

FIG. 11: Higgs signal strengths $\mu_{b\bar{b}}$ for the process $e^+e^- \to \nu_e\bar{\nu}_e H$ versus the mass $m_{Z'}$ for $\sqrt{s} = 500$ GeV (a) and $\sqrt{s} = 1000$ GeV (b) in the $B - L$ model.

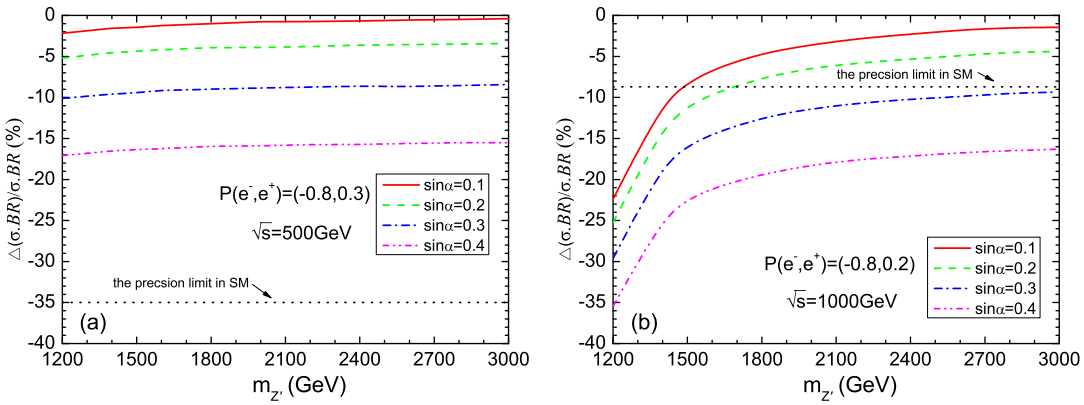

FIG. 12: Higgs signal strengths $\mu_{b\bar{b}}$ for the process $e^+e^- \to t\bar{t}H$ versus the mass $m_{Z'}$ for $\sqrt{s} = 500$ GeV (a) and $\sqrt{s} = 1000$ GeV (b) in the $B - L$ model.

expected at $\sqrt{s} = 500(1000)$ GeV. For $m_{Z'} \geq 2000$ GeV, sinα >0.1, the contributions of the $B - L$ model can be detected by the measurement of the $b\bar{b}$ signal rate at the ILC. From Table I one can see that at $\sqrt{s} = 500$ GeV, the accuracy for top Yukawa couplings is about 35%, which can be improved to the level of 8.7% at $\sqrt{s} = 1000$ GeV. Thus it is difficult to observe the $B - L$ effect on the process $e^+e^- \to t\bar{t}H$ at $\sqrt{s} = 500$ GeV via the $b\bar{b}$ channel. However, at $\sqrt{s} = 1000$ GeV, sin$\alpha \geq 0.1$, the absolute value of $b\bar{b}$ can deviate from the SM prediction by over 10%, which might be detected in the future ILC experiments.

In Fig. 13, we show the dependence of the Higgs signal strengths μ_{bb} on the parameter

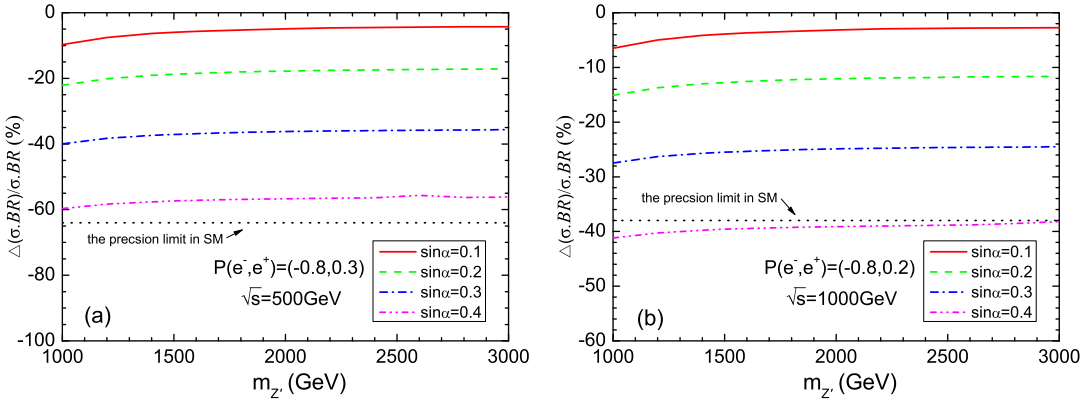

FIG. 13: Higgs signal strengths $\mu_{b\bar{b}}$ for the process $e^+e^- \to ZHH$ at $\sqrt{s} = 500$ GeV (a) and $e^+e^- \to \nu_e\bar{\nu}_e HH$ at $\sqrt{s} = 1000$ GeV (b) versus the mass $m_{Z'}$ in the $B-L$ model.

$m_{Z'}$ and sinα for the double Higgs production processes $e^+e^- \to ZHH$ and $e^+e^- \to \nu_e\bar{\nu}_e HH$ with polarized beams. We can see that in the allowed parameter space of the $B-L$ model, the Higgs signal strengths $\mu_{b\bar{b}}$ of the process $e^+e^- \to ZHH$ are below the expected precision of the ILC for $\sqrt{s}$=500 GeV. For the process $e^+e^- \to \nu_e\bar{\nu}_e HH$, we can see that this production channel will be hard to be observed at the ILC.

V. SUMMARY

Under current constraints, we investigated the single and double Higgs boson production processes $e^+e^- \to ZH$, $e^+e^- \to \nu_e\bar{\nu}_e H$, $e^+e^- \to t\bar{t}H$, $e^+e^- \to ZHH$ and $e^+e^- \to \nu_e\bar{\nu}_e HH$ in the $B-L$ model at the ILC. We calculated the production cross sections and the relative corrections with the polarized beams for $\sqrt{s}$=250 GeV, 500 GeV, 1000 GeV. We also studied the signal rates with the SM-like Higgs boson decaying to $b\bar{b}$, and performed a simulation by using the projected sensitivities given by ILC. For the three single Higgs boson production processes, in the reasonable parameter space, we found that the processes $e^+e^- \to ZH$ and $e^+e^- \to \nu_e\bar{\nu}_e H$ might approach the observable threshold of the ILC. For the two double Higgs boson production processes, we found that in most regions of parameter space, the Higgs signal strengths $\mu_{b\bar{b}}$ of them are all out of the observed threshold of the ILC so that the effects will be difficult to be observed at the ILC.

Acknowledgement

We would like to thank Lorenzo Basso and Alexander Belyaev for providing the CalcHep Model Code and the helpful suggestions. This work is supported by the Joint Funds of the National Natural Science Foundation of China under grant No. U1404113, by the Science and Technology Department of Henan province with grant No. 142300410043, by the National Natural Science Foundation of China under Grant Nos. 11405047, 11305049.

---

[1] ATLAS Collaboration, G. Aad et al., *Phys. Lett. B,* **716** (2012) 1.

[2] CMS Collaboration, S. Chatrchyan et al., *Phys. Lett. B,* **716** (2012) 30.

[3] S. Dawson, A. Gritsan, H. Logan et al., arXiv:1310.8361 [hep-ex]; T. Han, Z. Liu and J. Sayre, *Phys. Rev. D,* **89** (2014) 113006; M. E. Peskin, arXiv:1312.4974 [hep-ph]; P. Bechtle, S. Heinemeyer, O. Stal, T. Stefaniak, G. Weiglein, *JHEP,* **11** (2014) 039; C. Englert, A. Freitas, M. Muhlleitner et al., *J. Phys. G,* **41**, (2014) 113001.

[4] G. Aarons et al., [ILC Collaboration], arXiv:0709.1893 [hep-ph]; J. Brau et al., [ILC Collaboration], arXiv:0712.1950 [acc-ph]; T. Behnke, J. E. Brau, B. Foster et al., arXiv:1306.6327 [acc-ph].

[5] H. Baer et al., arXiv:1306.6352 [hep-ph]; D. M. Asner, T. Barklow, C. Calancha et al., arXiv:1310.0763 [hep-ph].

[6] see examples: Bernd A. Kniehl, *Int. J. Mod. Phys. A,* **17** (2002) 1457; F. Jegerlehner and O.Tarasov, *Nucl. Phys. Proc. Suppl,* **116** (2003) 83; G. Belanger et al., *Phys. Lett. B,* **559** (2003) 252; F. Boudjema et al., *Phys. Lett. B,* **600** (2004) 65; A. Denner, S. Dittmaier, M. Roth and M. M. Weber, *Phys. Lett. B,* **560** (2003) 196; *Nucl. Phys. Proc. Suppl,* **135** (2004) 88; A. Denner, S. Dittmaier, M. Roth, M. M. Weber, *Nucl. Phys. B,* **660** (2003) 289.

[7] H. Eberl, W. Majerotto and V. C. Spanos, *Phys. Lett. B,* **538** (2002) 353; *Nucl. Phys. B,* **657** (2003) 378; T. Hahn, S. Heinemeyer and G. Weiglein, *Nucl. Phys. B,* **652** (2003) 229; *Nucl. Phys. Proc. Suppl,* **116** (2003) 336; J. J. Cao et al., arXiv:1410.1018 [hep-ph].

[8] C. -X. Yue, S. Z. Wang, and D. Q. Yu, *Phys. Rev. D,* **68** (2003) 115004; C. -X. Yue, W. Wang, Z. J. Zong, and F. Zhang, *Eur. Phys. Jour. C,* **42** (2005) 331; X. L. Wang, Y. -B. Liu, J. H. Chen, H. Yang, *Eur. Phys. Jour. C,* **49** (2007) 593; S. L. Hu, N. Liu, J. Ren, L. Wu, *J. Phys. G,* **41**, (2014) 125004; N. Liu, J. Ren, L. Wu , P. W. Wu, J. M. Yang, *JHEP,* **04** (2014) 189; B. F. Yang, J. Z. Han, S. H. Zhou and N. Liu, *J. Phys. G,* **41**, (2014) 075009.

[9] L. Wang, W. Y. Wang, J. M, Yang, H. J. Zhang, *Phys. Rev. D,* **75** (2007) 074006; J. F. Shen, J. Cao and L. B. Yan, *Europhys. Lett,* **91** (2010) 51001; N. Liu, S. L. Hu, B. F. Yang, J. Z. Han, *Eur. Phys. Jour. C,* **01** (2015) 008; B. F. Yang, Z. Y. Liu, N. Liu, J. Z. Han, *Eur. Phys. Jour. C,* **74** (2014) 3203; B. F. Yang, J. Z. Han, N. Liu, *JHEP,* **04** (2015) 148; L. Wu, *JHEP,* **02** (2015) 061; Y.-B. Liu and Z.-J. Xiao, *J. Phys. G,* **42**, (2015) 065005; J. Z. Han, S. F. Li, B. F. Yang, N. Liu, *Nucl. Phys. B,* **896** (2015) 200.

[10] S. Khalil, *J. Phys. G,* **35**, (2008) 055001, arXiv:0611205 [hep-ph]; L. Basso, (Master Thesis, Universita' degli Studi di Padova, 2007).

[11] W. Emam and S. Khalil, *Eur. Phys. Jour. C,* **52** (2007) 625;

[12] L. Basso, A. Belyaev, S. Moretti, and C. H. Shepherd-Themistocleous, *Phys. Rev. D,* **80** (2009) 055030.

[13] L. Basso, A. Belyaev, S. Moretti, and G. M. Pruna, *JHEP,* **0910** (2009) 006.

[14] P. Fileviez Perez, T. Han, and T. Li, *Phys. Rev. D,* **80** (2009) 073015.

[15] L. Basso, arXiv:1106.4462 [hep-ph].

[16] L. Basso, S. Moretti, and G. M. Pruna, *Eur. Phys. Jour. C,* **71** (2011) 1724.

[17] L. Basso, S. Moretti and G. M. Pruna, *Phys. Rev. D,* **83** (2011) 055014.

[18] G. M. Pruna, arXiv:1106.4691 [hep-ph].

[19] C. Englert, T. Plehn, D. Zerwas, and P. M. Zerwas, *Phys. Lett. B,* **703** (2011) 298.

[20] V. V. Khoze and G. Ro, *JHEP,* **1310** (2013) 075.

[21] J. Hernández López and J. Orduz-Ducuara, *J. Phys. Conf. Ser.* **468**, (2013) 012012.

[22] R. Marshak and R. N. Mohapatra, *Phys. Lett. B,* **91** (1980) 222.

[23] R. N. Mohapatra and R. Marshak, *Phys. Rev. Lett,* **44** (1980) 1316.

[24] C. Wetterich, *Nucl. Phys. B,* **187** (1981) 343.

[25] A. Masiero, J. Nieves, and T. Yanagida, *Phys. Lett. B,* **116** (1982) 11.

[26] R. N. Mohapatra and G. Senjanovic, *Phys. Rev. D,* **27** (1983) 254.

[27] G. Cacciapaglia, C. Csaki, G. Marandella , A. Strumia, *Phys. Rev. D,* **74** (2006) 033011.

[28] K. A. Olive et al., [Particle Data Group collaboration], *Chin. Phys. C,* **38** (2014) 090001.

[29] Shankha Banerjee, Manimala Mitra, Michael Spannowsky, *Phys. Rev. D,* **92** (2015), 055013.

[30] A. Pukhov et al., arXiv:0412191 [hep-ph]; A. Belyaev, N. D. Christensen and A. Pukhov, *Comput. Phys. Commun.* **184**, (2013) 1729.

[31] G. Moortgat-Pick, T. Abe, G. Alexander et al., *Phys. Rept.,* **460** (2008) 131.

[32] A. Denner, J. Kublbeck, R. Mertig and M. Bohm, *Z. Phys. C,* **56** (1992) 261; C. Englert and M. McCullough, *JHEP,* **1307** (2013) 168.

[33] S. Dawson, A. Gritsan, H. Logan et al., arXiv:1310.8361 [hep-ex]; T. Han, Z. Liu and J. Sayre, arXiv:1311.7155 [hep-ph]; M. E. Peskin, arXiv:1312.4974 [hep-ph]; P. Bechtle et al., arXiv:1403.1582 [hep-ph].

[34] F. Goertz, A. Papaefstathiou, L. L. Yang and J. Zurita, *JHEP,* **1306** (2013) 016; R. S. Gupta, H. Rzehak and J. D. Wells, *Phys. Rev. D,* **88** (2013) 055024; A. J. Barr, M. J. Dolan, C. Englert and M. Spannowsky, *Phys. Lett. B,* **728** (2014) 308; V. Barger, L. L. Everett, C. B. Jack- son and G. Shaughnessy, *Phys. Lett. B,* **728** (2014) 433; D. E. F. de Lima, A. Papaefstathiou and M. Spannowsky, arXiv:1404.7139 [hep-ph].